Catalysis Today 164 (2011) 119–123

Contents lists available at ScienceDirect

Catalysis Today

journal homepage: www.elsevier.com/locate/cattod

Effect of reactant density inside supercages of zeolite La,Na-Y on the mechanism of the ethylbenzene conversion

Yijiao Jiang [1], Jun Huang [2,*], Michael Hunger [1,*]

[1] Institute of Chemical Technology, University of Stuttgart, D-70550 Stuttgart, Germany
[2] Laboratory for Catalysis Engineering, School of Chemical and Biomolecular Engineering, The University of Sydney, NSW 2006, Australia

ARTICLE INFO

Article history:
Available online 3 November 2010

Keywords:
Zeolite La,Na-Y
Acid catalyzed reaction
Ethylbenzene disproportionation
Reaction mechanism
Solid-state NMR spectroscopy

ABSTRACT

Zeolites La,Na-Y are important catalysts for industrial FCC units due to their acidic properties and stability. The ethylbenzene disproportionation on this zeolite was suggested as a standard test reaction for acidic zeolites by the Catalysis Commission of the International Zeolite Association (IZA). The present work provides solid-state ^{13}C NMR spectroscopic evidence that various amounts of reactants inside the supercages of zeolites La,Na-Y obviously affect the catalytic behavior of ethylbenzene reaction. At 453 K, diphenylethane was only detected on zeolite La,Na-Y with three ethylbenzene molecules per supercage. This intermediate, however, did not occur on samples with low loading (1 or 2 EB molecules per supercage). On zeolite La,Na-Y loaded with one molecule ethylbenzene per supercage, dealkylation and realkylation of ethylbenzene occurred at 548 K without any side-reactions. However, side-reactions of oligomerization, hydride transfer, and aromatization were observed on samples with high ethylbenzene loading, which promotes the catalyst deactivation. In addition, the zeolites La,Na-Y with high loadings of ethylbenzene show a higher reactivity and more complex reaction mechanisms.

1. Introduction

Lanthanum exchange of zeolites is an important procedure for the preparation of stable zeolite catalysts with enhanced acidity, e.g., for applications in cracking processes and alkylation reactions [1]. The dissociation of water molecules in the electrostatic fields of multivalent extra-framework lanthanum cations in zeolites results in the formation of LaOH groups bound to the extra-framework cations and bridging OH groups (SiOHAl) acting as Brønsted acid sites [2–5]. The type, number, and strength of acid sites on zeolites strongly depend on the dehydration temperature during activation [3–8]. By suitable tuning of the dehydration temperature, the properties of catalytically active sites can be adjusted to promote a desired reaction [9,10].

Disproportionation of aromatic hydrocarbons is an important acid catalyzed petrochemical reaction [11]. Ethylbenzene disproportionation into benzene and diethylbenzene has attracted much attention, because *p*-diethylbenzene has a high industrial potential in the recovery of *p*-xylene in the Parex and Eluxyl process [12]. In addition, the ethylbenzene disproportionation was suggested as a standard reaction for the characterization of Brønsted acidic zeolites by the International Zeolite Association (IZA) [13]. After reaching steady state conditions, the rate of the ethylbenzene disproportionation can be correlated with the number of strong Brønsted acid sites on zeolite catalysts [14–25]. In addition, this reaction is a shape selective reaction on zeolites. The reaction shows an induction period on large-pore zeolites and no induction period on medium-pore zeolites. Two main reaction pathways were proposed: (i) the diphenylethane-mediated reaction pathway on large-pore zeolites (Scheme 1) and (ii) the ethyl-transfer reaction pathway on medium-pore zeolites (Scheme 2) [11].

During ethylbenzene conversion on FAU-type zeolites, various loadings of the catalysts corresponding to various numbers of ethylbenzene molecules inside the supercages affect the reaction mechanism and, therefore, the final yield of desired products [14]. Till now, there are no detailed studies on the reaction mechanism of ethylbenzene disproportionation on FAU-type zeolites as a function of the reactant loading. Solid-state NMR spectroscopy is powerful to detect the reaction pathways inside zeolite pores without to modify the reaction system [26]. The present work describes solid-state ^{13}C NMR investigations of the ethylbenzene conversion on zeolite La,Na-Y with various loadings of 1, 2 or 3 ethylbenzene molecules per supercage at different reaction temperatures. The study gives new insights into the mecha-

* Corresponding authors. Tel.: +61 2 935 17483; fax: +61 2 935 12854.
E-mail addresses: jun.huang@sydney.edu.au (J. Huang), michael.hunger@itc.uni-stuttgart.de (M. Hunger).

0920-5861/$ – see front matter © 2010 Elsevier B.V. All rights reserved.
doi:10.1016/j.cattod.2010.10.024

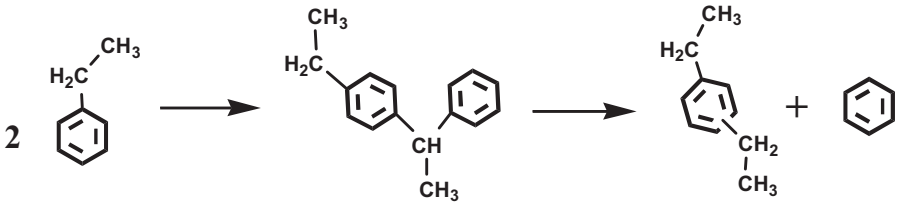

Scheme 1.

nism of this reaction and promotes its application as a standard reaction for characterization of acidic zeolites and in chemical industry.

2. Experimental

Zeolite La,Na-Y ($n_{Si}/n_{Al} = 2.7$) with ion-exchanged ratio of 73% was prepared as described elsewhere [7,27]. This zeolite catalyst was characterized by XRD and ^{27}Al and ^{29}Si MAS NMR spectroscopy, indicating that the obtained materials were neither damaged nor dealuminated. By quantitative ^{1}H MAS NMR measurements, the concentration of Brønsted acid sites (SiOHAl groups) located in the supercages of zeolite La,Na-Y dehydrated at 673 K for 12 h in vacuum was determined to *ca.* 1 SiOHAl per supercage.

For the present study, the zeolites were filled into a glass tube and subjected to activation in vacuum with the heating rate of 20 K/h up to the final temperature of 673 K. At this temperature, the zeolites were evacuated to below 10^{-2} mbar for 12 h. According to the weight of zeolites inside the tube, the number of SiOHAl in supercages was calculated for chemical loading. By adjusting the vapor pressure on a Schlenk line, ^{13}C-enriched ethyl[α-^{13}C]benzene (^{13}C-enrichment of 99%, purchased from Dr. Ehrenstorfer) was quantitatively loaded with 1, 2 or 3 molecules per supercage of zeolite La,Na-Y. The eventual error in calculation and experiment for loading was less than 10%. Subsequently, these samples were sealed in glass tubes. The heating of the sealed samples was performed in an external oven, while the solid-state NMR studies were carried out at room temperature.

^{13}C MAS NMR investigations were performed with a 7 mm Bruker MAS NMR probe on a Bruker MSL-400 spectrometer at the resonance frequency of 100.6 MHz. ^{13}C high-power proton decoupling (HPDEC) MAS NMR spectra were recorded after an excitation with a $\pi/2$ pulse and with the repetition time of 5 s. Sample spinning rates of *ca.* 4 kHz were applied. All solid-state ^{13}C NMR spectra were referenced to tetramethylsilane (TMS).

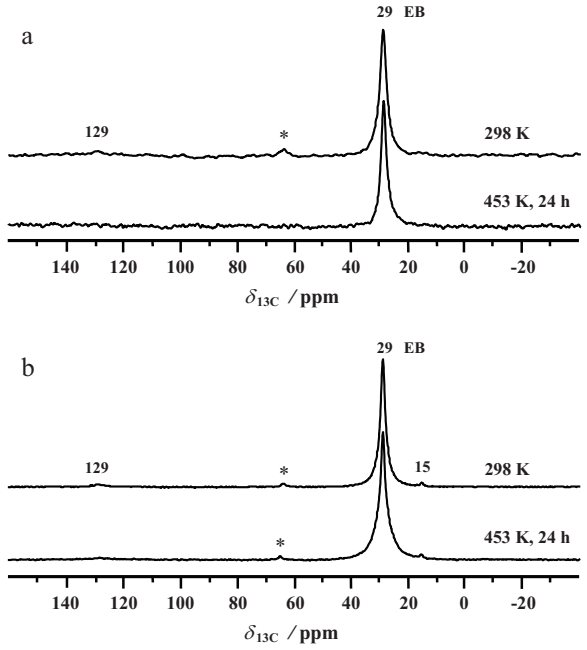

Fig. 1. ^{13}C MAS NMR spectra of ethyl[α-^{13}C]benzene conversion on zeolite La,Na-Y loaded with 1 molecule (a) and 2 molecules per supercage (b) and recorded after heating at 298–453 K. Asterisks denote spinning sidebands.

3. Results and discussion

3.1. Ethylbenzene conversion on zeolite La,Na-Y loaded with different amounts of reactant and after heating at 453 K

After adsorption of ethyl[α-^{13}C]benzene on zeolite La,Na-Y at 298 K, the ^{13}C MAS NMR spectra shown in Figs. 1 and 2 are dominated by a peak at 29 ppm due to the ^{13}C-enriched methylene group

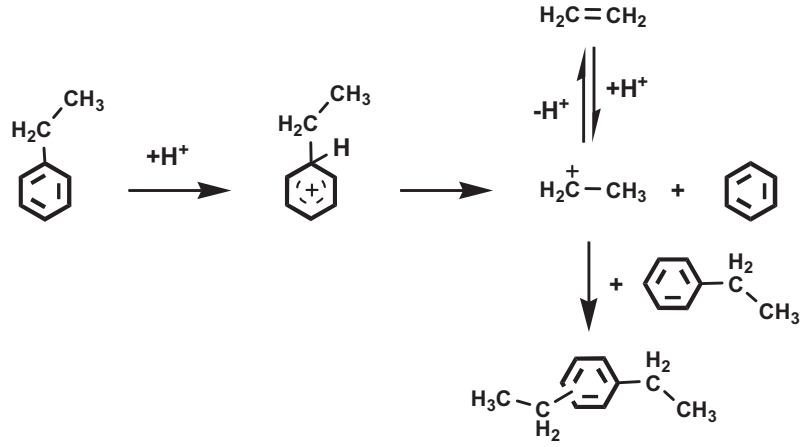

Scheme 2.

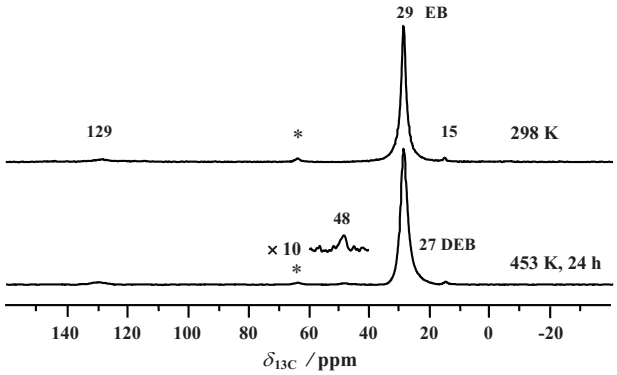

Fig. 2. ^{13}C MAS NMR spectra of ethyl[α-^{13}C]benzene conversion on zeolite La,Na-Y loaded with 3 molecules per supercage and recorded after heating at 298–453 K. Asterisks denote spinning sidebands.

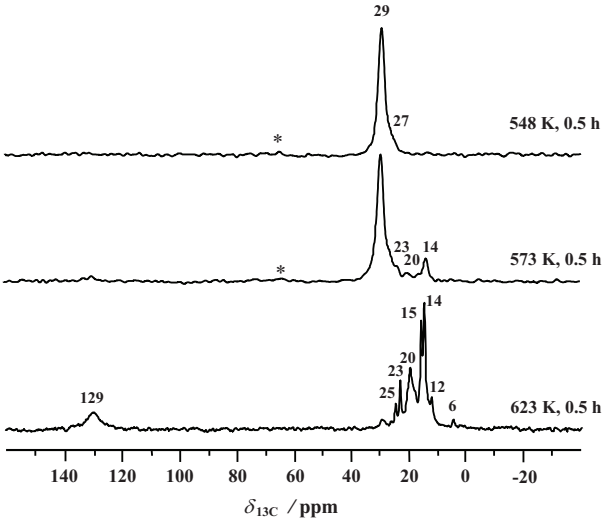

Fig. 3. ^{13}C MAS NMR spectra of ethyl[α-^{13}C]benzene conversion on zeolite La,Na-Y loaded with 1 molecule per supercage and recorded after heating at 548–623 K. Asterisks denote spinning sidebands.

of ethylbenzene. Two weak signals at 15 and 129 ppm are assigned to the non-enriched carbon atoms of the methyl group and the aromatic ring, respectively [9,10,28]. No conversion of ethylbenzene was observed at 298 K. However, the ^{13}C MAS NMR signals at 29 ppm in the spectra of Figs. 1 and 2 are much broader than the signal of the enriched methylene group of ethylbenzene adsorbed on zeolite H,Na-Y (see Ref. [10]). It should be noted that zeolites La,Na-Y and H,Na-Y were prepared from the same parent material. Therefore, both zeolites La,Na-Y and H,Na-Y should have similar entropic effects for ethylbenzene, which can not contribute for the broader signals.

Highly charged metal cations are Lewis acid sites, which always act as strong adsorption sites and can polarize the C—H bonds and even activate alkanes by hydride abstraction [29]. In a recent study, the three-fold charged extra-framework aluminum cations on the aluminum-exchanged zeolites caused a strong interaction with the side-chain of ethylbenzene resulting in the broadening of the ^{13}C MAS NMR signals [10]. Therefore, it can be expected that also the extra-framework lanthanum cations in zeolite La,Na-Y strongly interact with the ethyl groups of adsorbate molecules and contribute to the broadening of the signals at 29 ppm in Figs. 1 and 2. According to recent in situ pulsed-flow ^{1}H MAS NMR-UV/Vis study, the existence of Lewis acidic metal cations promotes the formation of sec-ethylphenyl carbenium ions by hydride abstraction of ethylbenzene [30].

Upon heating of all three samples at 453 K for 24 h, a new ^{13}C MAS NMR signal occurred at 48 ppm in Fig. 2 for zeolite La,Na-Y with high ethylbenzene loading (3 molecules per supercage). This signal is due to the formation of diphenylethane, which was also detected during ethylbenzene reactions on aluminum-exchanged zeolites X and Y [10]. This observation indicates that highly charged metal cations cause a polarizing effect on the C—H bonds of the methylene group of ethylbenzene and the subsequent transalkylation of two reactants to diphenylethane. However, the formation of diphenylethane was not observed for zeolite La,Na-Y loaded with one and two molecules ethylbenzene per supercage after heating at 453 K as shown in Fig. 1, and also not for zeolite H—Y loaded with ethylbenzene and heated under same conditions. On zeolite H—Y, a signal of diethylbenzene appeared at 27 ppm occurred in the ^{13}C MAS NMR spectrum recorded after the reaction at 453 K [10]. Diethylbenzene is also produced on zeolite La,Na-Y, but this signal is overlapped by the broad signal at 29 ppm.

Figs. 1 and 2 show that the different loadings of the zeolite catalysts with reactants obviously influence the reaction mechanism inside the supercages. According to investigation of the H/D exchange between various zeolites and ethylbenzene, the activation energy for the protonation of aromatic ring is *ca.* 40 kJ/mol [27], but the energy for activation of C—H bond at ethyl group was found to be *ca.* 200 kJ/mol [30]. If hydroxyl protons are available for the intermediate diphenylethane formed inside the supercage, it would be rapidly split to diethylbenzene and benzene. Due to the high energy barriers for the activation of ethylbenzene side-chain, the rate of the formation of diphenylethane species would be much lower than that of the scission. Zeolite La,Na-Y used as acidic catalyst in the present study contains *ca.* 1 SiOHAl per supercage. For the zeolite La,Na-Y loaded with three ethylbenzene molecules per supercage, two of them are involved in the reaction at 453 K to form diphenylethane. Since there are more ethylbenzene molecules than SiOHAl groups (3:1) in the supercages, all Brønsted acid sites are covered by adsorbate molecules. Therefore, the aromatic rings of the intermediate diphenylethane are not rapidly protonated and split, which results in a long lifetime of diphenylethane species allowing their observation at 48 ppm in the ^{13}C MAS NMR spectrum (Fig. 2).

3.2. Ethylbenzene conversion on zeolite La,Na-Y loaded with different amounts of reactant and after heating at 548–623 K

The investigation of ethylbenzene disproportionation on zeolite La,Na-Y described in the former section evidences that this reaction occurs at 453 K *via* the bimolecular reaction pathway (Scheme 1). When heating the ethylbenzene-loaded zeolite La,Na-Y at temperatures higher than 548 K, however, the pathway of ethylbenzene conversion is changed (Figs. 3–5). Already, earlier H/D exchange studies on acidic zeolite Y demonstrated that dealkylation and realkylation of ethylbenzene may occur at 523 K [30]. After heating zeolite La,Na-Y loaded with two or more ethylbenzene molecules per supercage at 548 K, there are new signals at 14–20 ppm in the ^{13}C MAS NMR spectra shown in Figs. 4 and 5. These signals are due to methyl carbons of oligomeric species [31,32]. The occurrence of these signals indicates that the dealkylation of ethylbenzene takes place. After adsorption of ethylbenzene on zeolites, the aromatic ring is rapidly protonated to form the ethylcyclohexadienyl carbenium ion. At higher temperatures, the activation energy for the dealkylation is reached and this carbocation is dealkylated to an ethyl group and a benzene molecule. If the ethyl group contacts a second ethylbenzene, diethylbenzene is formed. Otherwise, the above-mentioned carbocations are deprotonated to ethylene and transformed, subsequently, to oligomeric species. The formation of oligomeric species is considered as a

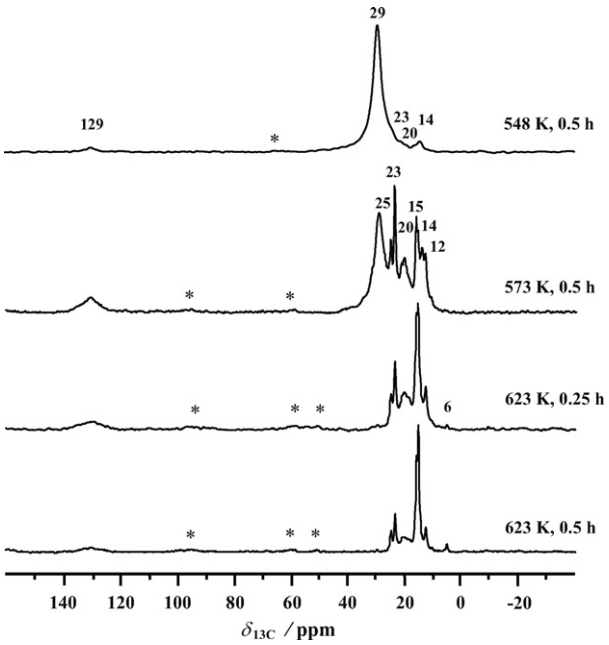

Fig. 4. ^{13}C MAS NMR spectra of ethyl[α-^{13}C]benzene conversion on zeolite La,Na-Y loaded with 2 molecules per supercage and recorded after heating at 548–623 K. Asterisks denote spinning sidebands.

hint to the monomolecular reaction mechanism of ethylbenzene disproportionation.

On zeolite La,Na-Y loaded with only one ethylbenzene molecule per supercage and heated at 548 K, however, the signal at 14–20 ppm due to oligomeric species could not be observed (Fig. 3). In this case, the ethyl cations have less chance to interact with each other for oligomerization because of the lower amount of ethylbenzene molecules per supercage. However, the highly active ethyl cation can react with a second ethylbenzene molecule to form diethylbenzene (27 ppm) or with a benzene molecule for realkylation to ethylbenzene. Surprisingly, there are no side-reactions for ethylbenzene disproportionation *via* a monomolecular reaction pathway (Scheme 2) on zeolite La,Na-Y with low reactant loading, which is interesting for industrial applications due to a lower production of by-products and a short reaction time.

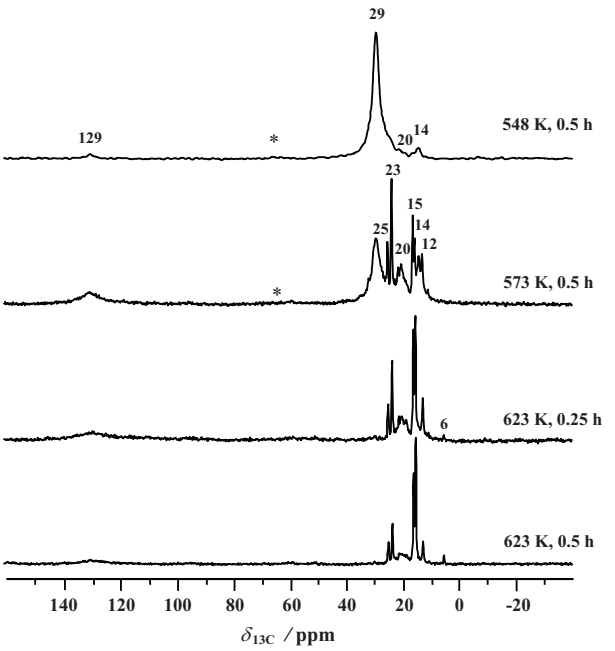

Fig. 5. ^{13}C MAS NMR spectra of ethyl[α-^{13}C]benzene conversion on zeolite La,Na-Y loaded with 3 molecules per supercage and recorded after heating at 548–623 K. Asterisks denote spinning sidebands.

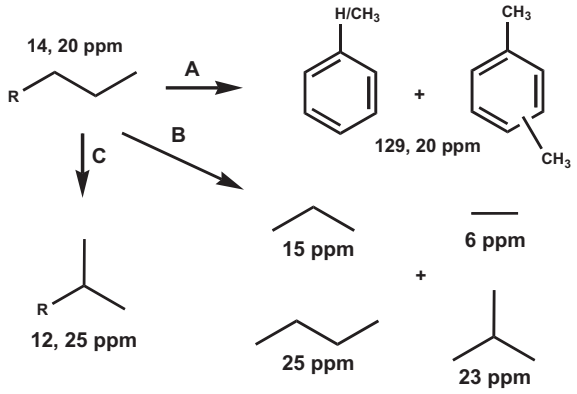

Scheme 3.

Further increasing of the reaction temperature for zeolite La,Na-Y loaded with one ethylbenzene molecule per supercage to 573 K, ^{13}C MAS NMR signals at 14–23 ppm occur (Fig. 3). In comparison with highly loaded zeolites La,Na-Y showing the formation of oligomeric species already at 548 K (Figs. 4 and 5), the formation of similar reaction products on the low loaded sample requires heating at 573 K. Highly loaded La,Na-Y zeolites produce more ethyl cations per supercage, leading to a faster generation of oligomeric species. In the case of the low-loaded sample, a higher reaction temperature is necessary for reaching a faster diffusion of the ethyl cations as a pre-requisite of oligomerization.

It should be noted that the formation of oligomeric species causing the signal at 14 ppm is always accompanied by the occurrence of other by-products, such as butane (23 ppm), toluene/xylene (methyl group at 20 ppm), and propane (15 ppm) as demonstrated by the ^{13}C MAS NMR spectra shown in Figs. 3–5. This observation indicates that the oligomerization reaction induces addition side-reactions, such as hydride transfer, aromatization reactions, and cracking.

In Scheme 3, three reaction pathways **A**, **B**, and **C** are proposed. According to pathway **A**, oligomeric species (14 ppm) are firstly transferred into cyclohexanyl cations after six-ring closure. During a series of deprotonation and hydride transfer steps, cyclohexene species are produced. Subsequently, these cyclohexene species contact alkylcarbenium ions to form cyclohexenyl cations and alkanes (C_3 and C_4 hydrocarbon at 15 and 23 ppm) by the intermolecular hydride transfer. Repetition of these heterogeneously catalyzed reactions results in the formation of toluene/xylene (20 and 129 ppm).

The increase of the ^{13}C MAS NMR signal at 129 ppm due to aromatic compounds formed by ethylbenzene conversion on zeolite La,Na-Y, as shown in Figs. 3–5, is much less than earlier observed for ethylbenzene conversion on H-ZSM-5 (see Ref. [9]). On the other hand, the signals at 12, 15, 23, and 25 ppm in Figs. 3–5 show significant intensities. Therefore, ethylbenzene reactions on La,Na-Y prefer pathways **B** and **C** of Scheme 3. Increase of the reaction temperature to 623 K or prolongation of the reaction time (Figs. 3–5, bottom) lead to strong ^{13}C MAS NMR signals of propane and ethane molecules formed *via* pathway **B**. According to this pathway, oligomeric species are cracked into *n*-butane (25 ppm), *i*-butane (23 ppm), propane (15 ppm), and ethane (6 ppm) *via* a protolytic cracking on the Brønsted acid sites. Zeolite La,Na-Y has supercages with enough space for the formation of large reaction intermediates allowing the isomerization of hydrocarbons inside

the cages. Therefore, skeletal isomerization of oligomeric cations and other carbocations occurs, which leads to the formation of isoalkanes responsible for the ^{13}C MAS NMR signals at 12 and 25 ppm in Figs. 3–5.

Generally, the density and strength of Brønsted acid sites on zeolites have significant effects on the reaction rate of ethylbenzene disproportionation, which is the reason why it was suggested by the IZA as test reaction for acidic zeolites. Comparing the experimental results obtained for the same zeolite catalyst with different amounts of the reactant ethylbenzene per supercage (Figs. 3–5), the reactivity and selectivity of the reaction system was found to change with the ethylbenzene loading. This is essential to select suitable reaction conditions for ethylbenzene disproportionation as a test reaction for acidic zeolites and for industrial applications.

4. Conclusions

The ethylbenzene disproportionation on zeolite La,Na-Y was suggested by the Catalysis Commission of the International Zeolite Association (IZA) as a standard reaction for the characterization of acidic zeolites. During this reaction, an induction period was observed taking more than 10 h at 453 K. During this induction period, formation of higher alkylated aromatics, such as ployalkylated diphenylethanes, occurs. The present study demonstrates that different amounts of ethylbenzene on zeolite La,Na-Y obviously influence the formation of diphenylethanes inside the supercages of this catalyst. By ^{13}C MAS NMR spectroscopy, the formation of diphenylethane could be exclusively observed for zeolite La,Na-Y loaded with three ethylbenzene molecules per supercage. For zeolite samples with lower ethylbenzene loading (1 or 2 molecules per supercage), not all Brønsted acidic SiOHAl groups are covered by adsorbate molecules and are available for the further conversion of reaction intermediates, i.e., rapid splitting, due to the low activation energy of this reaction. For all samples, extra-framework lanthanum cations on zeolite La,Na-Y worked as Lewis acid sites interacting with the ethyl groups of reactants and caused the broader signals in ^{13}C MAS NMR spectra.

Increasing of the reaction temperatures to 548 K led to dealkylation and realkylation of ethylbenzene on zeolite La,Na-Y. Interestingly, no oligomerization and other side-reactions could be observed for the zeolite sample loaded with one molecule per supercage. However, side-reactions of oligomerization, hydride transfer, and aromatization were found for zeolite samples loaded with two and three ethylbenzene molecules per supercage. These side-reactions promoted the catalyst deactivation and caused the slow decreasing of the conversion as a function of time-on-stream during catalytic reactions. Upon ethylbenzene conversion at 548 and 623 K, the zeolites La,Na-Y samples loaded with larger amounts of ethylbenzene show the higher reactivity, but also the more complex reaction network. This is essential for selecting suitable conditions for ethylbenzene disproportionation as catalytic test reaction and for industrial applications.

Acknowledgments

We thank Deutsche Forschungsgemeinschaft and Volkswagen-Stiftung Hannover for financial support.

References

[1] J. Weitkamp, L. Puppe, Catalysis and Zeolites—Fundamentals and Application, Springer-Verlag, Berlin, 1999.
[2] A.E. Hirschler, Journal of Catalysis 2 (1963) 428.
[3] E.F.T. Lee, L.V.C. Rees, Zeolites 7 (1987) 545.
[4] E.F.T. Lee, L.V.C. Rees, Zeolites 7 (1987) 446.
[5] E.F.T. Lee, L.V.C. Rees, Zeolites 7 (1987) 143.
[6] J. Huang, Y. Jiang, V.R.R. Marthala, B. Thomas, E. Romanova, M. Hunger, Journal of Physical Chemistry C 112 (2008) 3811.
[7] J. Huang, Y. Jiang, V.R. Marthala, Y.S. Ooi, J. Weitkamp, M. Hunger, Microporous and Mesoporous Materials 104 (2007) 129.
[8] A. Guzman, I. Zuazo, A. Feller, R. Olindo, C. Sievers, J.A. Lercher, Microporous and Mesoporous Materials 83 (2005) 309.
[9] J. Huang, Y. Jiang, V.R.R. Marthala, A. Bressel, J. Frey, M. Hunger, Journal of Catalysis 263 (2009) 277.
[10] J. Huang, Y. Jiang, V.R.R. Marthala, M. Hunger, Journal of the American Chemical Society 130 (2008) 12642.
[11] G. Ertl, H. Knözinger, J. Weitkamp, Handbook of Heterogeneous Catalysis, Wiley-VCH, Weinheim, Germany, 1997.
[12] R.V. Jasra, S.G.T. Bhat, Separation Science and Technology 23 (1988) 945.
[13] D.E. De Vos, S. Ernst, C. Perego, C.T. O'Connor, M. Stöcker, Microporous and Mesoporous Materials 56 (2002) 185.
[14] N. Arsenova-Hartel, H. Bludau, W.O. Haag, H.G. Karge, Microporous and Mesoporous Materials 35–6 (2000) 113.
[15] N. Arsenova, H. Bludau, W. Haag, H.G. Karge, Microporous and Mesoporous Materials 23 (1998) 1.
[16] H.G. Karge, S. Ernst, M. Weihe, U. Weiss, J. Weitkamp, Studies in Surface Science and Catalysis 84 (1994) 1805.
[17] J. Weitkamp, S. Ernst, P.A. Jacobs, H.G. Karge, Erdol & Kohle Erdgas Petrochemie 39 (1986) 13.
[18] W.W. Kaeding, Journal of Catalysis 95 (1985) 512.
[19] H.G. Karge, Y. Wada, J. Weitkamp, P.A. Jacobs, Journal of Catalysis 88 (1984) 251.
[20] M. Guisnet, Journal of Catalysis 88 (1984) 249.
[21] H.G. Karge, Z. Sarbak, K. Hatada, J. Weitkamp, P.A. Jacobs, Journal of Catalysis 82 (1983) 236.
[22] H.G. Karge, K. Hatada, Y. Zhang, R. Fiedorow, Zeolites 3 (1983) 13.
[23] H.G. Karge, J. Ladebeck, Z. Sarbak, K. Hatada, Zeolites 2 (1982) 94.
[24] M. Weihe, M. Hunger, M. Breuninger, H.G. Karge, J. Weitkamp, Journal of Catalysis 198 (2001) 256.
[25] U. Weiss, M. Weihe, M. Hunger, H.G. Karge, J. Weitkamp, Studies in Surface Science and Catalysis 105 (1997) 973.
[26] M. Hunger, W. Wang, Advances in Catalysis 50 (2006) 149.
[27] J. Huang, Y.J. Jiang, V.R.R. Marthala, W. Wang, B. Sulikowski, M. Hunger, Microporous and Mesoporous Materials 99 (2007) 86.
[28] A. Philippou, M.W. Anderson, Journal of Catalysis 167 (1997) 266.
[29] G. Busca, Chemical Reviews 107 (2007) 5366.
[30] J. Huang, Y.J. Jiang, V.R.R. Marthala, Y.S. Ooi, M. Hunger, Chemphyschem 9 (2008) 1107.
[31] A.G. Stepanov, M.V. Luzgin, V.N. Romannikov, V.N. Sidelnikov, E.A. Paukshtis, Journal of Catalysis 178 (1998) 466.
[32] W. Wang, J. Jiao, Y.J. Jiang, S.S. Ray, M. Hunger, Chemphyschem 6 (2005) 1467.